

1           **Evaluation of efficiency and sensitivity of 1D and 2D sample**  
2           **pooling strategies for diagnostic screening purposes**

3  
4           **Jasper Verwilt<sup>1,2,3</sup>, Pieter Mestdagh<sup>1,2,3,4</sup>, Jo Vandesompele<sup>1,2,3,4</sup>**

5                           *1 OncoRNALab, Cancer Research Institute Ghent*

6           *2 Department of Biomolecular Medicine, Faculty of Medicine and Health Sciences,*

7   *Ghent University*

8                           *3 Center for Medical Genetics, Ghent University*

9   *4 Biogazelle, Belgium*

10  
11       **Abstract**

12   As SARS-CoV-2 continues to spread around the world while the pandemic lasts,  
13   testing facilities are forced to massively increment their testing capacities to handle  
14   the increasing number of samples. While sample pooling methods have been  
15   proposed or are effectively implemented in some labs, no systematic and large-scale  
16   simulations have been performed using real-life quantitative data from testing  
17   facilities. Here, we use anonymous data from 1632 positive cases to simulate and  
18   compare 1D and 2D pooling strategies. We show that the choice of pooling method  
19   and pool size is an intricate decision with a prevalence-dependent efficiency-  
20   sensitivity trade-off.

## 25 **Introduction**

26 Massive screening of the population for SARS-CoV-2 infection is proposed as one of  
27 the key strategies in the global battle against the COVID-19 pandemic. Due to the  
28 immense number of samples that are analyzed during population screening, pooling  
29 of samples seems to be a valid strategy in overcoming shortages in reagents and  
30 increasing testing capacity.

31

32 Several pooling strategies in the frame of SARS-CoV-2 testing have been discussed  
33 in recent preprints. The most discussed method is referred to as one-time pooling<sup>1-4</sup>.

34 In this strategy, the samples are pooled, pools are tested and only samples in

35 positive pools are tested individually. A second popular approach is called sequential

36 pooling<sup>1,5</sup> in which the samples are pooled, pools are tested and positive pools are

37 split into two equally-sized sub-pools. These sub-pools are tested again and this

38 process is repeated until the individual sample level is reached. The third method that

39 has been explored is two-dimensional or 2D pooling<sup>6</sup>. This method organizes

40 samples in a 2D matrix and then creates pools along the rows and columns of the

41 matrix. The pools are tested and negative rows and columns are excluded from the

42 matrix. Next, all remaining samples are tested individually. Finally, researchers have

43 explored pooling strategies in which samples are assigned to multiple pools, but

44 require only one round of testing. Given the composition and test results of the

45 positive pools, the positive samples can immediately be identified without the need

46 for further individual testing. P-BEST<sup>7</sup> and Tapestry<sup>8</sup> are examples of such strategies.

47

48 While attractive, pooling strategies come with inherent limitations. First, pooling

49 dilutes each individual sample, possibly to such an extent that the viral RNA

50 becomes undetectable, resulting in false negative observations<sup>9-11</sup>. A second  
51 limitation is that an increase in sample manipulations augments the risk of cross-  
52 contamination and sample mix-ups, which can lead to false negatives and false  
53 positives<sup>6</sup>. Other drawbacks are unique to specific strategies. The P-BEST pooling  
54 protocol is very time consuming, even when using a pipetting robot<sup>7</sup>. The repeated  
55 pooling method, on the other hand, suffers from a complicated re-pooling scheme<sup>1</sup>.

56

57 Although the number of preprints and peer-reviewed publications on pooling  
58 strategies for COVID-19 PCR-based testing has increased rapidly throughout the  
59 pandemic, some important insights are still lacking. First of all, the proposed optimal  
60 pooling strategy is often based on a binary classification of samples as either positive  
61 or negative. However, this Boolean approach is not in accordance with the real-world  
62 situation and does not allow for investigating the dilution effect of pooling. Second,  
63 when using a quantitative representation of the viral loads, these values need to  
64 reflect real-life data, as patients present a very wide range of viral loads. This is  
65 reflected in the wide spectrum of Cq values reported by PCR-based tests<sup>12</sup>. Finally,  
66 as pooling is most effective for population-wide screening (where a very low  
67 prevalence is expected) it is important to determine the performance of strategies  
68 when encountering a low fraction of positive samples.

69

70 Here, we evaluate one-time (or 1D) pooling and two-dimensional (2D) pooling (using  
71 practical microtiter plate format pool sizes) as promising strategies for massive, low-  
72 prevalence population screening using real-life RT-qPCR data from 1632 positive  
73 samples.

74

## 75 **Results**

### 76 *Inverse relationship between efficiency and prevalence*

77 In order to evaluate the efficiency-gain of the adopted pooling strategies, we  
78 calculated the number of tests that are needed to analyze all samples and divided  
79 this number by the total number of samples. We calculated the median, minimum  
80 and maximum prevalence-specific efficiency for each pooling strategy (Figure 1).  
81 First, we observe an inverse relationship between efficiency and prevalence over the  
82 evaluated prevalence range from 0.01% to 10% for all pooling strategies. Second,  
83 there is no single most efficient strategy, because this depends on the prevalence  
84 (notice crossings in Figure 1). Until a prevalence of 0.36%, 1x24 is the most efficient  
85 strategy, from 0.40% to 2.51% 16x24 becomes the most efficient, from 2.82% to  
86 4.47% the most efficient strategy is 12x24 and from 5.01% to 10% 8x12 is the most  
87 efficient strategy. However, at high prevalence all strategies show similar efficiency  
88 gain. Third, strategies employing a larger pool size display a higher efficiency when  
89 the prevalence is low, but as the prevalence increases, there is a tipping point for  
90 each strategy at which its smaller pool size variant becomes more efficient. At very  
91 low prevalence, the efficiency of a 1 x  $n$  pool size becomes  $n$  and that of a  $m$  x  $n$  pool  
92 strategy becomes  $(m \times n) / (m + n)$ . As a general trend, 2D pooling methods are less  
93 sensitive to changes in prevalence in comparison with 1D pooling methods. We  
94 conclude that the most efficient pool size very much depends on the prevalence, but  
95 2D pooling methods generally are most efficient when prevalence is higher than  
96 0.4%.

97

98 *Sensitivity decreases with lower prevalence*

99 The true performance of a pooling strategy cannot be evaluated by efficiency only.  
100 Since the number of false negatives due to pooling is one of the main possible  
101 drawbacks of sample pooling, it is necessary to take this into account when choosing  
102 the optimal strategy. In this regard, we calculated the average sensitivity of the  
103 different simulated settings (Figure 2, Supplemental Figure 3), which ranges from  
104 0.636 to 0.968. For all of the pooling strategies—and irrespective of pool size—we  
105 primarily see that sensitivity increases with increasing prevalence. There is a non-  
106 linear relationship between sensitivity and prevalence. Furthermore, since prevalence  
107 is linked with efficiency and as a result indirectly linked with sensitivity, we note that  
108 an increase in efficiency comes with a decrease in sensitivity. We also observe that  
109 at a prevalence lower than 1%, there is an increased variation in sensitivity for  
110 different simulation cohorts. Thus, the increased efficiency at low prevalence comes  
111 with a low and pool size-dependent problematically variable sensitivity.

112

### 113 *Sensitivity loss in function of viral load*

114 With the intention of determining the influence of the viral load and, as a proxy, Cq  
115 value of the positive sample on the sensitivity associated with the pooling strategies,  
116 we calculated the probabilities of a true-positive for each non-pooled original Cq  
117 value (Supplemental Figure 2). We investigated how the sensitivity changes when  
118 higher Cq values are progressively being included in the cohort, starting with  
119 samples with highest viral load (lowest Cq value) (Figure 3, Supplemental Figure 4).  
120 In the first place, we note that the Cq value at which sensitivity loss starts to occur  
121 only depends on the 1D pool size or largest dimension of the 2D pool; i.e. Cq value  
122 of 35 for 1x4, 34 for 1x8, 33.4 for 1x12 and 8x12, 33 for 1x16 and 12x16 and 32.4 for  
123 1x24 and 16x24. These Cq values are (as expected) identical to

124  $37 - \log_2(\text{largest pool size})$ . Additionally, when Cq values larger than these cut-off  
125 values are systematically included, the sensitivity drops exponentially. The rate at  
126 which this reduction happens, decreases when prevalence increases. Finally, when  
127 the prevalence is 10%, larger pool sizes result in a smaller reduction in sensitivity,  
128 but for all other visualized prevalence values the sensitivity decreases with larger  
129 pool size. Altogether, the extent to which low viral load samples contribute to the drop  
130 in sensitivity depends on pool size and pooling strategy, although the sensitivity  
131 decrease is most problematic when prevalence is low.

132

## 133 **Discussion**

134 Sample pooling strategies form an incredible asset in an attempt to increase  
135 throughput in times when massive testing for COVID-19 would be needed. A plethora  
136 of pooling strategies have been suggested, some more performant or practical than  
137 others. 1D and 2D pooling methods were selected in this simulation study because  
138 they are simple and quick to perform, have straightforward pipetting schemes and do  
139 not require re-accessing the same sample more than twice. Pool sizes were selected  
140 to be easily compatible with 96-well plates. Using a large real-life dataset of 1632  
141 positive samples enabled us to simulate relevant settings and provide more accurate  
142 outcomes in comparison with real wet-lab tests, which are rather limited in the  
143 number of positive samples and may not cover the whole range of viral loads.  
144 Because the original Cq distribution depends on the origin of the sample (hospital,  
145 care center, ...) and the stage of pandemic, our observations do as well. Firstly, our  
146 results confirm the widely accepted idea that sample pooling methods show a higher  
147 efficiency when prevalence is low<sup>1-6,13</sup> and that, for 1D and 2D pooling methods, as  
148 prevalence increases, a threshold is reached after which smaller pool sizes become

149 more efficient<sup>1,6</sup>. However, appraising the performance of a pooling method  
150 exclusively by its efficiency would ignore one of the major drawbacks of pooling: loss  
151 of sensitivity due to dilution of the target. This issue becomes most pertinent when  
152 the viral load is low<sup>9-11,13,14</sup>. Our results confirm that all tested pooling methods suffer  
153 from false negatives, to a variable degree (Figure 2). This loss in sensitivity across all  
154 prevalence conditions generally precludes use of pooling for diagnostic testing of  
155 COVID-19 samples according to the U.S. Food and Drug Administration (FDA),  
156 whereby only 1x16 and 1x24 strategies under high prevalence ( $\geq 10\%$ ) conditions  
157 meet the minimal 95% sensitivity requirement<sup>15</sup>. When prevalence is high, the loss in  
158 sensitivity for large pools is partly compensated by the fact that low viral load  
159 samples can be ‘rescued’ by high viral load samples when present in the same pool.  
160 (Figure 3). Intuitively, 2D pooling methods are especially vulnerable for false  
161 negatives, as a high Cq sample would have to be ‘rescued’ in the corresponding row  
162 and column pools, which is confirmed by our results. The influential role of  
163 prevalence on efficiency as well as sensitivity presents an import challenge,  
164 considering that, in order to make an informed decision on the preferential pooling  
165 strategy, the prevalence has to be known. By nature, we cannot know the exact  
166 prevalence before testing our samples, and as a result, the prevalence has to be  
167 estimated. In general, we show that it is of extreme importance that an optimal  
168 equilibrium between efficiency and sensitivity is achieved when deciding on the  
169 pooling strategy and corresponding pool size.

170

## 171 **Materials and Methods**

172 *Patient samples*

173 Nasopharyngeal swabs were taken by a healthcare professional as a diagnostic test  
174 for SARS-CoV-2, as part of the Belgian national testing platform. The individuals  
175 were tested at nursing homes or in triage centers, between April 9<sup>th</sup> and June 7<sup>th</sup>. To  
176 mimic low prevalence viral loads as much as possible, only batches of 94 patient  
177 samples with fewer than 10 positives were included in this study. After additional  
178 filtering as described in a further paragraph, this resulted in 113 928 patients in total,  
179 of which 1632 positives (1.43%) with corrected Cq values ranging from 9.85 to 36.94  
180 (median of 28.78) (Supplemental Figure 1).

181

#### 182 *SARS-CoV-2 RT-qPCR test*

183 RNA extraction was performed using the Total RNA Purification Kit (Norgen Biotek  
184 #24300) according to the manufacturer's instructions using 200 µl transport medium,  
185 200 µl lysis buffer and 200 µl ethanol, with processing using a centrifuge (5810R with  
186 rotor A-4-81, both from Eppendorf). RNA was eluted from the plates using 50 µl  
187 elution buffer (nuclease-free water), resulting in approximately 45 µl eluate. RNA  
188 extractions were simultaneously performed for 94 patient samples and 2 negative  
189 controls (nuclease-free water). After addition of the lysis buffer, 4 µl of a proprietary  
190 700 nucleotides spike-in control RNA (40 000 copies) and carrier RNA (200 ng of  
191 yeast tRNA (Roche #10109517001) was added to all 96 wells from the plate). To the  
192 eluate of one of the negative control wells, 7500 RNA copies of positive control RNA  
193 (Synthetic SARS-CoV-2 RNA Control 2, Twist Biosciences #102024) were added.

194 Six µl of RNA eluate was used as input for a 20 µl RT-qPCR reaction in a CFX384  
195 qPCR instrument using 10 µl iTaq one-step RT-qPCR mastermix (Bio-Rad  
196 #1725141) according to the manufacturer's instructions, using 250 nM final  
197 concentration of primers and 400 nM of hydrolysis probe. Primers and probes were



198 synthesized by Integrated DNA Technologies using clean-room GMP production. For  
199 detection of the SARS-CoV-2 virus, the Charité E gene assay was used (FAM)<sup>16</sup>; for  
200 the internal control, a proprietary hydrolysis probe assay (HEX) was used. Prior to  
201 May 25th, 2 singleplex assays were performed; after May 25th, 1 duplex RT-qPCR  
202 was performed (with 1/8<sup>th</sup> of spike-in control RNA). Cq values were generated using  
203 the FastFinder software v3.300.5 (UgenTec). Only batches were approved with a  
204 clean negative control and a positive control in the expected range.

205

#### 206 *Assembly of positive Cq value distribution*

207 First, a subset of full 96-well RNA plates is selected containing less than 10 positives.  
208 The latter selection criterium is introduced to filter out plates originating from high  
209 COVID-19 positive rate circumstances, such as hospitals, to avoid putative bias  
210 towards high viral loads. Only plates are retained with a positive control value that is  
211 within two standard deviations of the mean positive control value of all filtered plates.  
212 Next, in order to correct the Cq values for inter-plate variation, the difference of the  
213 average positive control Cq values per qPCR plate from the overall mean positive  
214 control Cq is calculated. The Cq values in each qPCR plate are then corrected by the  
215 qPCR plate-specific difference from the mean. Supplemental Figure 1 displays the  
216 distribution of the corrected Cq values of the positive samples. Finally, by inspecting  
217 this histogram, we dismiss all Cq values larger than 37 as noisy data, resulting in a  
218 final set of 1632 positive Cq values.

219

#### 220 *Simulation of 1D and 2D pooling strategies*

221 Simulations of are run using R 4.0.1. First, several cohorts of 100 000 patients are  
222 repeatedly simulated with varying fractions  $f$ , defined by  $f = 10^{-x}$  with  $x =$

223 4, 3.95, ..., 1, of positive cases (resulting in 61 cohorts of 0.01% to 10% prevalence).  
224 This is done five times, resulting in five replicate cohort per prevalence (302 cohorts).  
225 The Cq values of the positive samples are sampled with replacement from the set of  
226 1632 positive Cq values. Next, the patients are randomly separated into pools  
227 depending on the pooling strategy that is simulated. The pooling strategies that were  
228 simulated are 1x4, 1x8, 1x12, 1x16, 1x24 (all 1D), and 8x12, 12x16 and 16x24. The  
229 Cq value of the pool was calculated as follows:

230

$$c_{pool} = \log_2 P - \log_2 \sum_{i=1}^p 2^{-c_i}$$

231

232 With  $c_{pool}$  the Cq value of the pool,  $P$  the number of samples in the pool,  $p$  the  
233 number of positive samples in the pool,  $c_1, c_2, \dots, c_p$  the Cq values of the positive  
234 samples. If the Cq value of the pool is smaller than 37, it is classified as a positive  
235 pool. For 1D pooling, only samples in positive pools are retained and the remaining  
236 individual Cq values were checked to be positive. For 2D pooling, the Cq values of  
237 the differently sized pools are checked simultaneously and the samples in negative  
238 pools are removed, after which all Cq values of the remaining samples are checked  
239 individually. Samples that were retained after the testing of the pools and had an  
240 individual Cq lower than 37 are classified as positive, all other samples are classified  
241 as negative.

242 The sensitivity is calculated as:

243

$$sensitivity = \frac{\# \text{ true positive samples}}{\# \text{ true positive samples} + \# \text{ false negative samples}}$$

244

245 The analytical efficiency gain is calculated as:

246

$$efficiency\ gain = \frac{\# \text{ tests required for individual testing}}{\# \text{ tests required for pooling strategy}}$$

247

248 In all simulations, the number of tests required for individual testing is equal to the  
249 number of samples.

250

## 251 **Acknowledgements**

252 We are grateful for the data from the Belgian federal taskforce for COVID-19 qPCR  
253 testing.

254

## 255 **Authors' contributions**

256 Conceptualization: J.Va., P.M. and J.Ve.; Methodology: J.Va., P.M. and J.Ve.;  
257 Software: J.Ve.; Formal Analysis: J.Ve.; Resources: J.Va. and P.M.; Data Curation:  
258 J.Ve.; Writing – Original Draft: J.Va. and J.Ve.; Writing – Review & Editing: J.Va.,  
259 P.M. and J.Ve.; Visualisation: J.Va. and J.Ve.; Supervision: J.Va and P.M.; Project  
260 Administration: J.Va. and P.M.

261

## 262 **Data availability**

263 The code and Cq values are available on  
264 <https://github.com/jasperverwilt/covidpooling>. The Cq values are available as an  
265 RDML file in the RDMLdb database<sup>17</sup>, under ID 2008AA74.

266

## 267 **References**

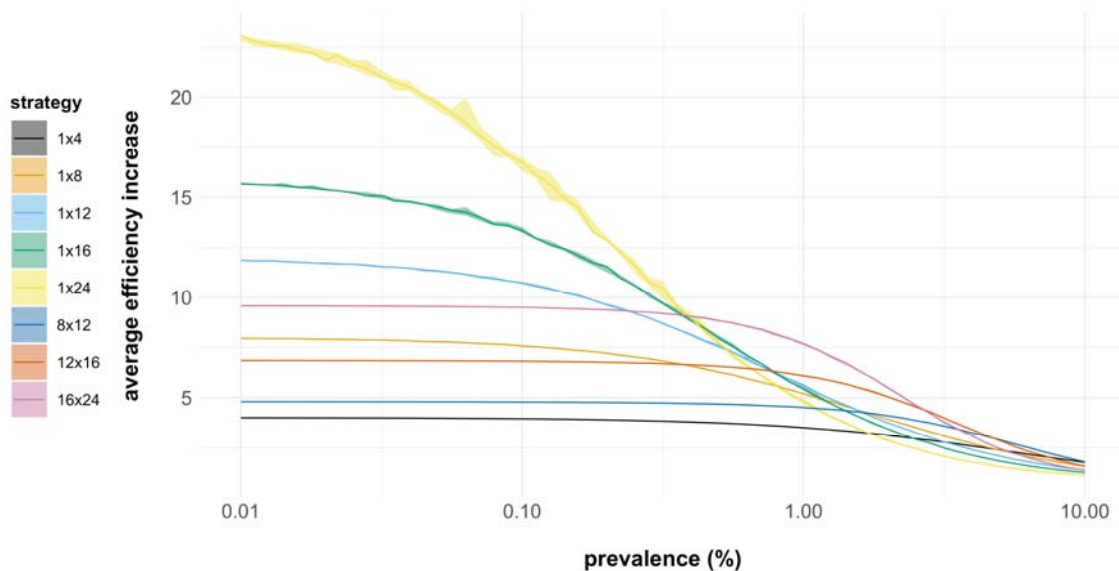
- 268 1. Shani-Narkiss, H., Gilday, O. D., Yayon, N. & Landau, I. D. Efficient and  
269 Practical Sample Pooling High-Throughput PCR Diagnosis of COVID-19.  
270 *medRxiv* 2020.04.06.20052159 (2020). doi:10.1101/2020.04.06.20052159
- 271 2. Guha, P., Guha, A. & Bandyopadhyay, T. Application of pooled testing in  
272 screening and estimating the prevalence of Covid-19. *medRxiv*  
273 2020.05.26.20113696 (2020). doi:10.1101/2020.05.26.20113696
- 274 3. Adams, K. Expanding Covid-19 Testing: Mathematical Guidelines for the  
275 Optimal Sample Pool Size Given Positive Test Rate. *medRxiv*  
276 2020.05.21.20108522 (2020). doi:10.1101/2020.05.21.20108522
- 277 4. Millionni, R. & Mortarino, C. Sequential informed pooling approach to detect  
278 SARS-CoV2 infection. *medRxiv* 2020.04.24.20077966 (2020).  
279 doi:10.1101/2020.04.24.20077966
- 280 5. Bukhari, S. U. K., Khalid, S. S., Syed, A. & Shah, S. S. H. Smart Pooled  
281 sample Testing for COVID-19: A Possible Solution for Sparsity of Test Kits.  
282 *medRxiv* 2020.04.21.20044594 (2020). doi:10.1101/2020.04.21.20044594
- 283 6. Sinnott-Armstrong, N., Klein, D. & Hickey, B. Evaluation of Group Testing for  
284 SARS-CoV-2 RNA. *medRxiv* 2020.03.27.20043968 (2020).  
285 doi:10.1101/2020.03.27.20043968
- 286 7. Shental, N. *et al.* Efficient high throughput SARS-CoV-2 testing to detect  
287 asymptomatic carriers. *medRxiv* 2020.04.14.20064618 (2020).  
288 doi:10.1101/2020.04.14.20064618
- 289 8. Ghosh, S. *et al.* Tapestry: A Single-Round Smart Pooling Technique for  
290 COVID-19 Testing. *medRxiv* 2020.04.23.20077727 (2020).  
291 doi:10.1101/2020.04.23.20077727
- 292 9. Torres, I., Albert, E. & Navarro, D. Pooling of Nasopharyngeal Swab

- 293           Specimens for SARS-CoV-2 detection by RT-PCR. *medRxiv*  
294           2020.04.22.20075598 (2020). doi:10.1101/2020.04.22.20075598
- 295   10.   Yelin, I. *et al.* Evaluation of COVID-19 RT-qPCR test in multi-sample pools.  
296           *Clin. Infect. Dis.* (2020). doi:<https://doi.org/10.1093/cid/ciaa531>
- 297   11.   Gan, Y. *et al.* Sample Pooling as a Strategy of SARS-COV-2 Nucleic Acid  
298           Screening Increases the False-negative Rate. *medRxiv* 2020.05.18.20106138  
299           (2020). doi:10.1101/2020.05.18.20106138
- 300   12.   Liu, Y. *et al.* Viral dynamics in mild and severe cases of COVID-19. *The Lancet*  
301           *Infectious Diseases* **20**, 656–657 (2020).
- 302   13.   Ben-Ami, R. *et al.* Pooled RNA extraction and PCR assay for efficient SARS-  
303           CoV-2 detection. *medRxiv* 2020.04.17.20069062 (2020).  
304           doi:10.1101/2020.04.17.20069062
- 305   14.   Nguyen, N. T., Aprahamian, H., Bish, E. K. & Bish, D. R. A methodology for  
306           deriving the sensitivity of pooled testing, based on viral load progression and  
307           pooling dilution. *J. Transl. Med.* **17**, 252 (2019).
- 308   15.   U.S. Food and Drug Administration. *Molecular Diagnostic Template for*  
309           *Laboratories.* (2020).
- 310   16.   Corman, V. M. *et al.* Detection of 2019 novel coronavirus (2019-nCoV) by real-  
311           time RT-PCR. *Eurosurveillance* **25**, 2000045 (2020).
- 312   17.   Ruijter, J. M. *et al.* RDML-Ninja and RDMLdb for standardized exchange of  
313           qPCR data. *BMC Bioinformatics* **16**, (2015).

314

315

316 **Figures**



317

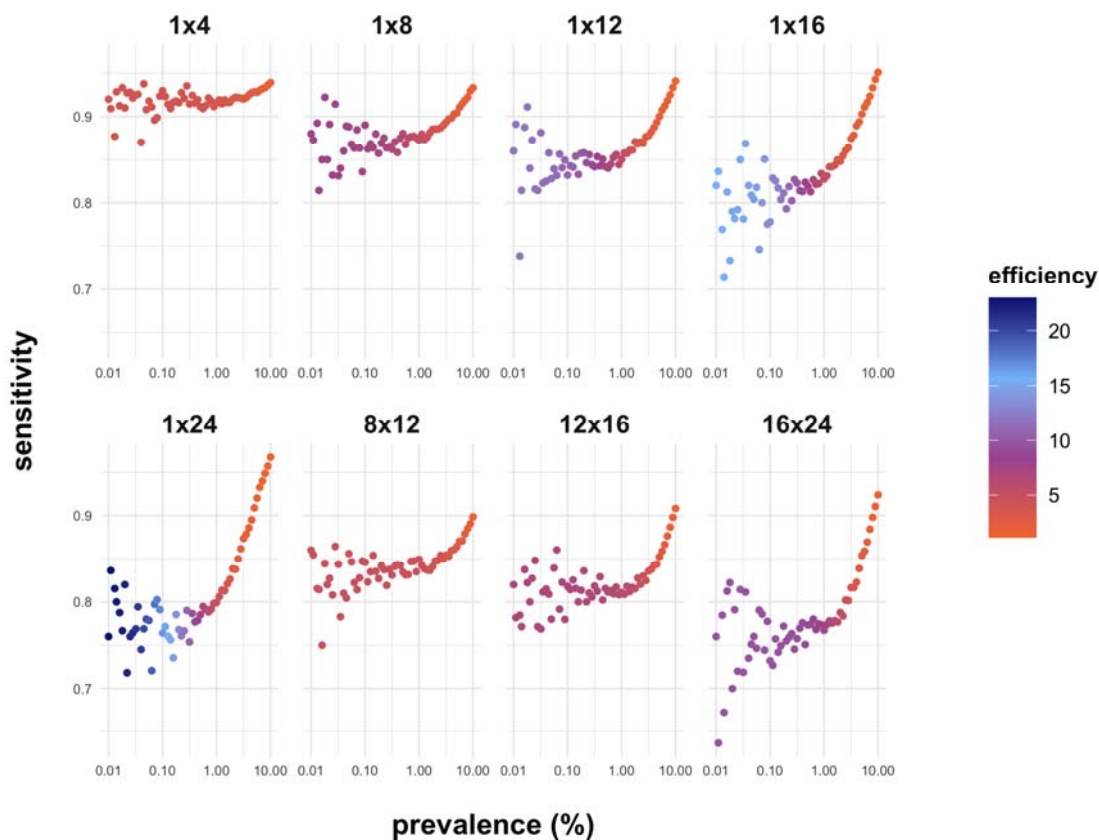
318 **Figure 1:** Average efficiency increase (number of samples divided by the number of tests performed)

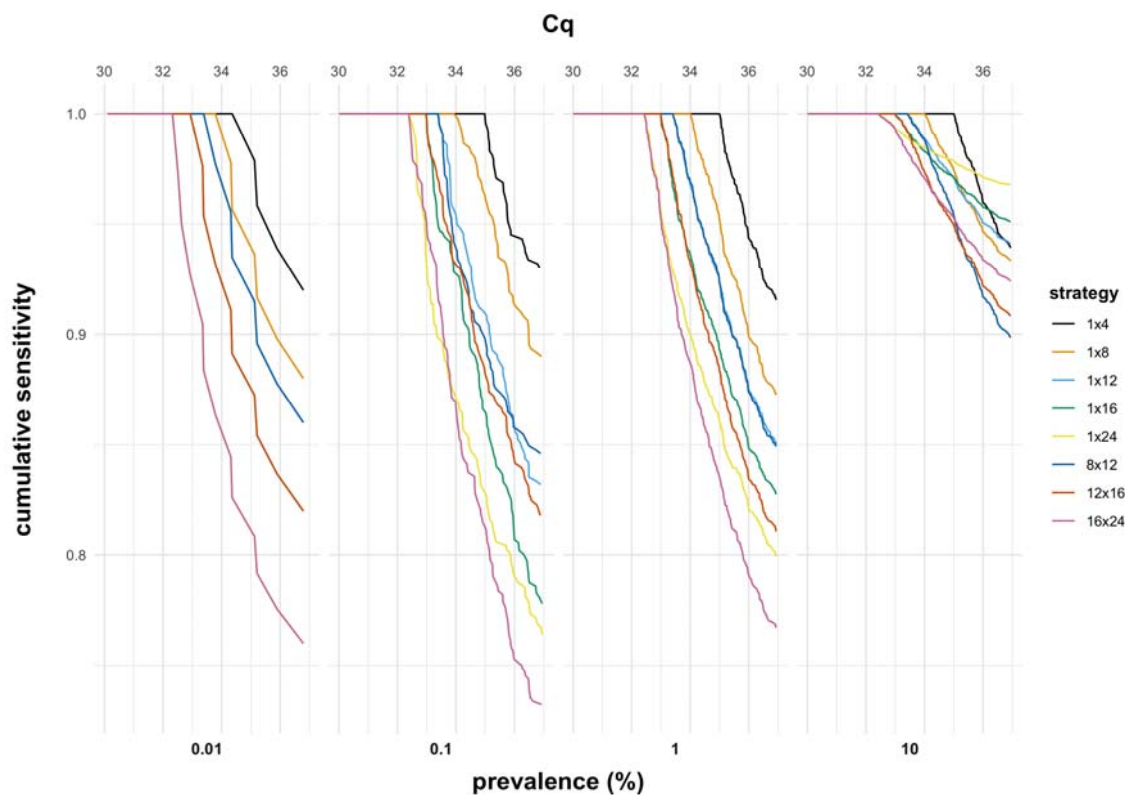
319 over a 0.01 to 10% prevalence range for different pooling strategies. The averages are approximated

320 by the median over five replicate simulations of a cohort size of 100 000 patients each. The ranges

321 around the line indicate the minimum and maximum value over five replicate simulations.

322





330

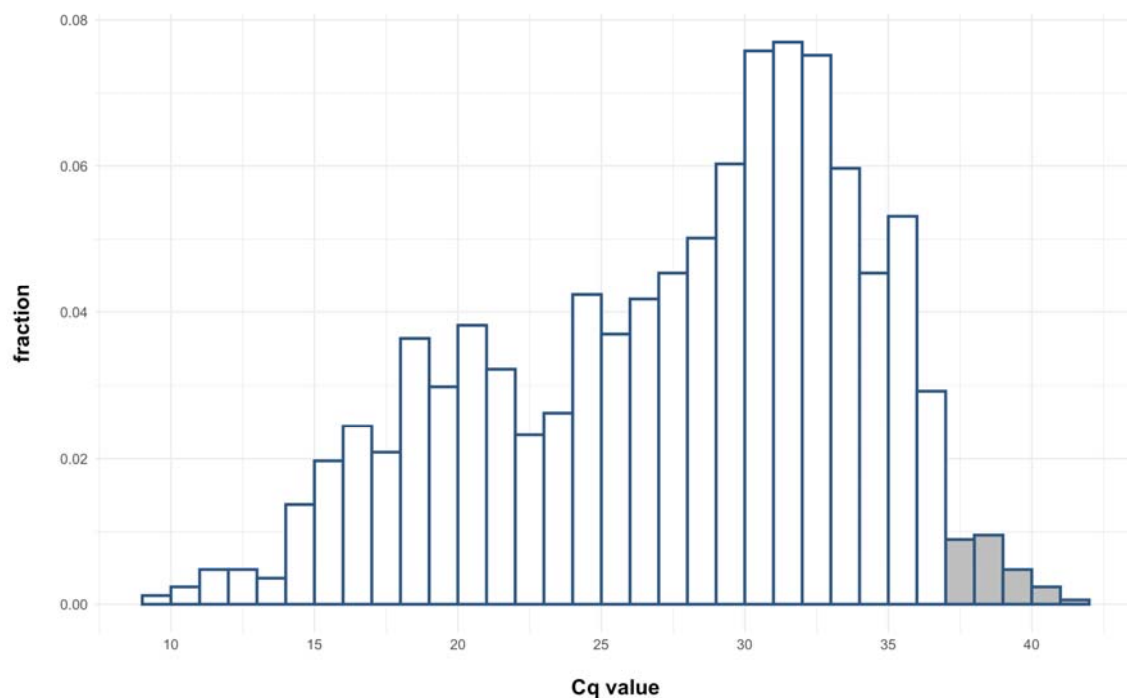
331 **Figure 3:** Cumulative sensitivities calculated for all Cq values up to a cut-off Cq for four prevalences.

332 All true positives and false negatives over five replicate simulations for each sampled Cq value are  
333 counted and used for calculation of the sensitivity up to the cut-off Cq. The data is filtered for  
334 prevalences of 0.01%, 0.1%, 1% and 10% and grouped by prevalence.

335



## 336 Supplemental Figures

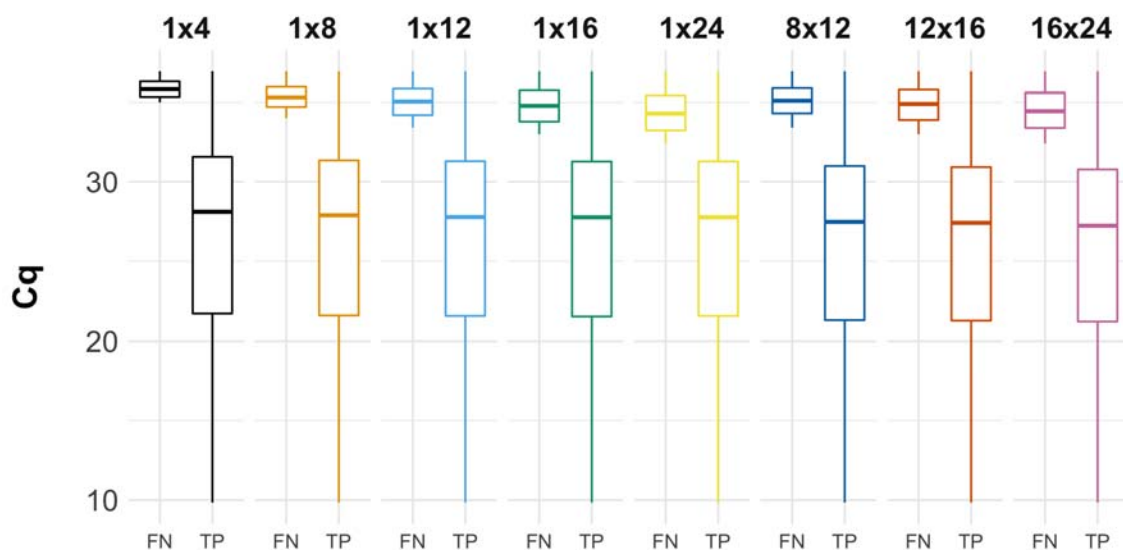


337

338 **Supplemental Figure 1:** The binned distribution of Cq values of all full 96-well RNA plates with good  
339 controls and less than 10 positives. The Cq values are corrected by calculating the difference between  
340 the mean positive control Cq value per 384-well qPCR plate from the overall mean of the positive  
341 control Cq values. Grey bars indicate the Cq values classified as noise.

342

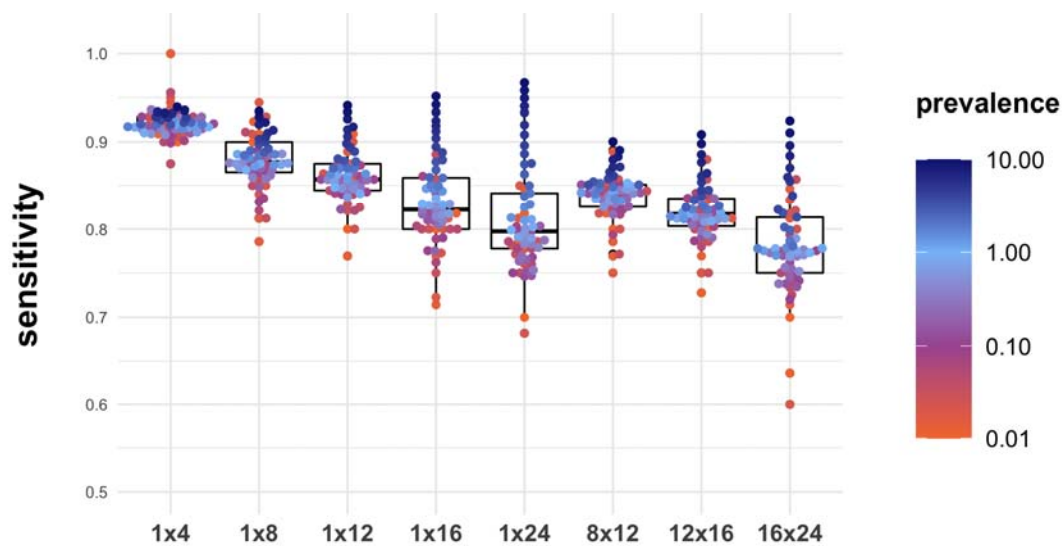
343



344

345 **Supplemental Figure 2:** Cq value distributions for false negatives (FN) and true positives (TP) for  
346 different pooling strategies. Each data point represents a Cq value from a replicate simulation with a  
347 set prevalence.

348

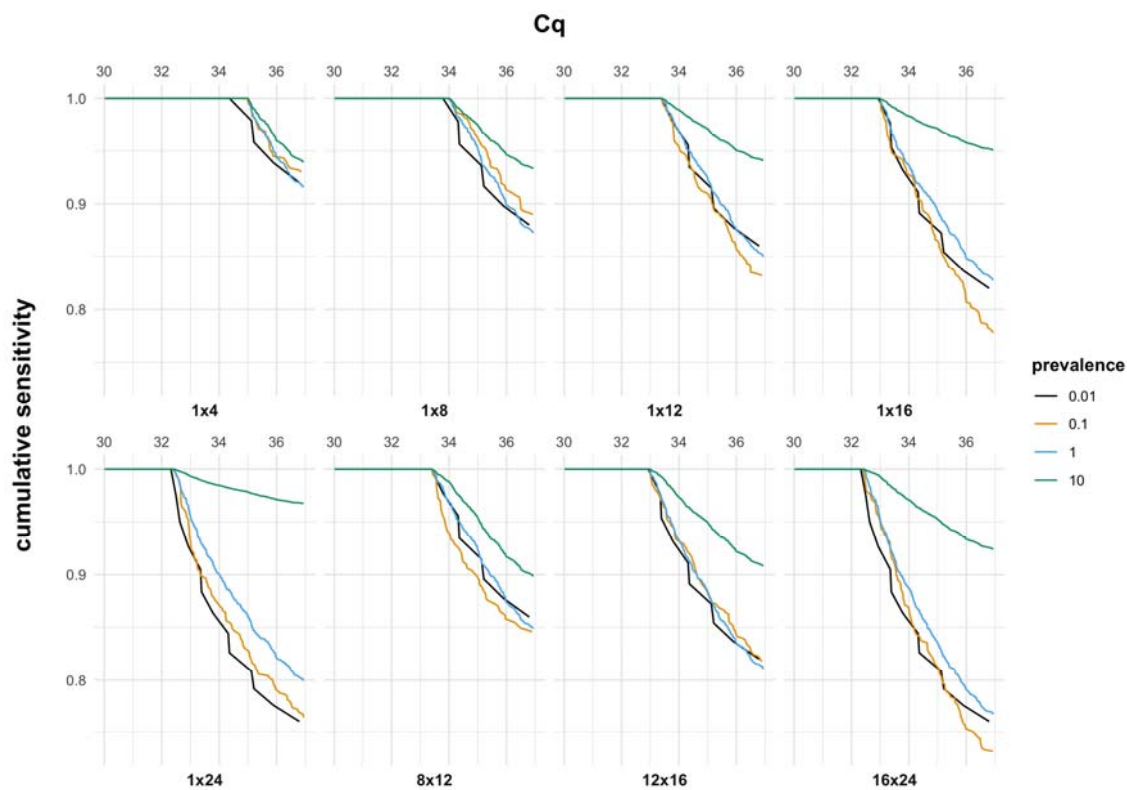


349

350 **Supplemental Figure 3:** Distributions of the average sensitivity for the simulations in each group.

351 Each data point is the median sensitivity over five simulations.

352



353

354 **Supplemental Figure 4:** Cumulative sensitivities calculated for all Cq values up to a cut-off Cq for  
355 each strategy. All true positives and false negatives over five replicate simulations for each sampled  
356 Cq value are counted and used for calculation of the sensitivity up to the cut-off Cq. The data is filtered  
357 for prevalences of 0.01%, 0.1%, 1% and 10% and colored accordingly.

358